Front. Optoelectron. 2013, 6(4): 429–434
DOI 10.1007/s12200-013-0342-x

RESEARCH ARTICLE

Improvement of blue InGaN light-emitting diodes with gradually increased barrier heights from n- to p-layers

Wu TIAN, Xiong HUI (✉), Yang LI, Jiangnan DAI, Yanyan FANG, Zhihao WU, Changqing CHEN

Wuhan National Laboratory for Optoelectronics, Huazhong University of Science and Technology, Wuhan 430074, China

Abstract The advantages of blue InGaN light-emitting diodes (LED) with the active region of gradually increased barrier heights from n- to p-layers are studied. The energy band diagram, hole concentration, electrostatic field near the electron blocking layer (EBL), and the internal quantum efficiency (IQE) are investigated by Crosslight simulation program. The simulation results show that the structure with gradually increased barrier heights has better performance over the equal one, which can be attributed to the mitigated polarization effect near the interface of the last barrier/EBL due to less interface polarization charges. Moreover, reduced barrier height toward the n-layers is beneficial for holes injection and transportation in the active region. As a result, holes are injected into the active region more efficiently and distributed uniformly in the quantum wells, with which both the IQE and the total lighting power are increased. Although it can lead to the broadening of the spontaneous emission spectrum, the increase is slight such that it has little effect on the application in solid-state lighting.

Keywords InGaN, light-emitting diodes (LED), polarization effect, gradual barrier height

1 Introduction

In recent years, the III-nitride light-emitting diodes (LEDs) have received much attention because of their potential usages in ultraviolet and blue lighting and detection [1], high density optical storage systems, full-color displays, chemical sensors, and medical applications [2,3]. Specially, the InGaN LEDs are widely studied due to the advantages of wide spectrum coverage, low power consumption, compact size, and long lifetime over conventional incandescent and florescent lamps [4,5]. However, the quenching of current injection efficiency at high injection level is still a challenge to fabricating high-efficiency LED devices. This problem becomes especially prominent for InGaN LEDs, which limits their high power application. The mechanisms determining the current injection efficiency in general semiconductor LED and laser devices have been widely studied [6–8]. Various factors are proved to affect the injection process, such as carrier transport (mainly limited by hole transport), thermionic carrier escape processes [9,10], and recombinations in both quantum wells (QWs) and barrier layers. Thermionic carrier escape processes under high current injection are revealed to cause the current injection efficiency quenching in InGaN-based LEDs [11–13], which is consistent with recent experimental works [14,15].

On the other hand, III-nitride LEDs suffer from low hole injection efficiency. In a typical LED structure, a large number of holes remain at the interface of the electron blocking layer (EBL) and p-GaN, which attract electrons to flow over the EBL and thus reduce the radiative recombination rate. Therefore, to enhance the quantum efficiency and suppress the current injection quenching of InGaN LEDs, it is important to design a new structure which has high electron blocking and hole injection efficiency.

Several recent works have proposed the design of novel barrier structure for suppression of quantum efficiency droop in nitride-based LEDs, such as using large bandgap AlInN [7,9,11,12] or AlGaN [16] barrier materials, and gradually changing single barrier height [17]. Interband Auger process is also proved to have important contributions to efficiency droop [18]. A potential solution to this issue is using new active region materials instead of traditional QW materials [19]. Furthermore, other approaches have been proposed to improve the hole injection efficiency, such as grading barrier design for the EBL [20], using polarization matched AlInGaN EBL [21], specially designed AlGaN/GaN superlattice EBL [22], and

Received May 13, 2013; accepted June 24, 2013

E-mail: hsiung.hust@gmail.com

Mg doped multi-quantum wells (MQWs) for the active region [23]. Nonetheless, there are still drawbacks in these approaches, such as non-uniform distribution of holes in quantum wells and poor crystalline quality caused by dopant, which bring new challenges to the device performance.

In this work, the structure with gradually increased barrier heights from the n-layers to p-layers is proposed to overcome those drawbacks in current InGaN LEDs design. Crosslight APSYS (Advance Physical Model of Semiconductor Devices) programs, which solve the Schrödinger equation, Poisson's equation, the carrier transport equations, and the current continuity equation self-consistently [24], are used to simulate the band diagram, and the optical and electrical properties of the structure in details.

2 Sample structure and parameters

The LEDs labeled as structure A with equal barrier heights, shown in Fig. 1, is used as a reference. The proposed sample is labeled as structure B. Two-dimension finite element analysis is used for the simulation, and the device width is set to be 200 μm. These two structures are designed to be grown on a *c*-plane sapphire substrate, followed by a 1-μm-thick undoped GaN layer, and a 3-μm-thick n-type GaN layer (n doping = 5×10^{18} cm^{-3}). The active region of structure A includes three 2-nm-thick $In_{0.21}Ga_{0.79}N$ QWs separated by four 15-nm-thick GaN barriers, while the barrier heights of structure B are increased from n-type to p-type layers by varying the mole fraction of In and Al. A 20-nm-thick p-type $Al_{0.15}Ga_{0.85}N$ EBL (p doping = 5×10^{17} cm^{-3}) is on top of the active region, followed by a 500-nm-thick p-type GaN contact layer (p doping = 1.2×10^{18} cm^{-3}). The background doping

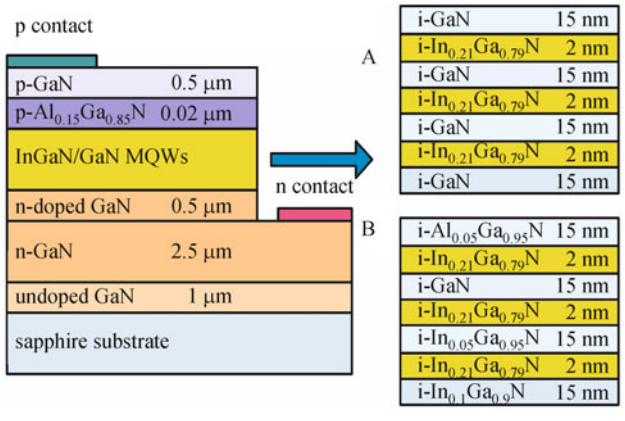

Fig. 1 Schematic diagrams of structures A and B. In structure A the three pairs of InGaN/GaN quantum wells are of uniform composition, while in structure B barrier heights are gradually increased toward p-AlGaN layer

levels for the undoped i-GaN, i-InGaN, and i-AlGaN layer used in the simulation are set to be 5×10^{16}, 1×10^{17}, and 1×10^{16} cm^{-3} [25], respectively. The main advantages of the proposed sample are expected to not only reduce polarization field near the interface between the last barrier and the EBL, but also change the distribution of electrons and holes in each QW. With the improvements, the carriers injection efficiency quenching can be mitigated. The Shockley-Read-Hall (SRH) recombination time is set to be 0.8 ns, and the internal loss is 2000 m^{-1} [26].

In general, the band gap energies of InGaN and AlGaN are governed by the following formulas [27]:

$$E_g(In_xGa_{1-x}N) = xE_{g,InN} + (1-x)E_{g,GaN} - b_1x(1-x),$$
$$E_g(Al_xGa_{1-x}N) = xE_{g,AlN} + (1-x)E_{g,GaN} - b_2x(1-x),$$

where $E_{g,InN}$, $E_{g,GaN}$, and $E_{g,AlN}$ are the band gap energies of InN, GaN and AlN, which equal to 0.77, 3.42 and 6.25 eV, respectively [27]. The bowing parameters b_1 and b_2 of InGaN and AlGaN are 3 and 1 eV respectively, and the band-offset ratio is assumed to be 0.7/0.3 for InGaN and AlGaN materials.

It is well known that AlN, GaN, InN and their crystal alloys crystallize are in the wurtzite structure with space group C_{6v}^4, which means that there are strong spontaneous polarization and piezoelectric polarization in the InGaN and AlGaN materials [25]. The highly polar nature yields a large amount of fixed charge at interfaces, which can induce a big electrostatic field in the LED. The total macroscopic polarization P of InGaN (AlGaN) is defined as the sum of the spontaneous polarization P_{SP} in the equilibrium lattice and the strain-induced piezoelectric polarization P_{PE}. The spontaneous polarization P_{SP_InGaN} (P_{SP_AlGaN}) can be obtained by numeric interpolations between the physical properties of GaN and InN (AlN) [28]:

$$P_{SP\_In_xGa_{1+x}N} = P_{SP}^{InN}x + P_{SP}^{GaN}(1-x) - \beta_1x(1-x),$$

$$P_{SP\_Al_xGa_{1+x}N} = P_{SP}^{AlN}x + P_{SP}^{GaN}(1-x) - \beta_2x(1-x),$$

where β_1 and β_2 are the bowing parameters, defined as -0.038 C/m^2 for InGaN and -0.019 C/m^2 for AlGaN. Piezoelectric polarizations of InGaN and AlGaN are dependent on the strains in the materials, which can be expressed as [29,30]:

$$P_{PE} = 2\frac{a(x)-a_0}{a_0}\left(e_{31} - e_{33}\frac{C_{13}}{C_{33}}\right),$$

where $a(x)$ and a_0 are the lattice constants of relaxed and pseudomorphically strained $In_xGa_{1-x}N$ ($Al_xGa_{1-x}N$), respectively; e_{31} and e_{33} are piezoelectric constants; and C_{13} and C_{33} are elastic constants of the $In_xGa_{1-x}N$ ($Al_xGa_{1-x}N$), which can also be obtained by the linear interpolation between the physical properties of GaN and

InN (AlN). The related parameters used in the programs are listed in Table 1, which can be found in Refs. [31,32]. Under polarization, the sheet charge density σ can be obtained by the following equation:

$$\sigma = (P_{SP} + P_{PE})_{top} - (P_{SP} + P_{PE})_{bottom}.$$

Taking into account the screening by defects, the surface charge densities are assumed to be 40% of the calculated values [33]. In structure A, the surface charge density is 7.8×10^{16} m^{-2} at the InGaN/GaN interface, and is 2.5×10^{16} m^{-2} at the interface between the last barrier and EBL. The fixed charge densities of structure B used in this program are shown in Table 2.

Table 1 Important parameters of AlN, GaN and InN used in the programs

parameters	GaN	AlN	InN
a/Å	3.189	3.112	3.545
c/Å	5.185	4.982	5.703
$m_{\parallel e}$	0.2	0.32	0.07
$m_{\perp e}$	0.2	0.3	0.07
C_{13}/GPa	106	108	92
C_{33}/GPa	398	373	224
e_{13}/(C·m^{-2})	−0.35	−0.5	−0.57
e$_3$/(C·m^{-2})	1.27	1.79	0.97
P_{SP}/(C·m^{-2})	−0.034	−0.09	−0.042

Table 2 Surface fixed charge densities at interfaces of structure B

interface	surface charge density/m^{-2}
i-In$_{0.1}$Ga$_{0.9}$N/i-GaN	-3.4×10^{16}
i-In$_{0.21}$Ga$_{0.79}$N/i-In$_{0.1}$Ga$_{0.9}$N	-4.4×10^{16}
i-In$_{0.05}$Ga$_{0.95}$N/i-In$_{0.21}$Ga$_{0.79}$N	6.1×10^{16}
i-In$_{0.21}$Ga$_{0.79}$N/i-In$_{0.05}$Ga$_{0.95}$N	-6.1×10^{16}
i-GaN/i-In$_{0.21}$Ga$_{0.79}$N	7.8×10^{16}
i-In$_{0.21}$Ga$_{0.79}$N/i-GaN	-7.8×10^{16}
i-Al$_{0.05}$Ga$_{0.95}$N/i-In$_{0.21}$Ga$_{0.79}$N	8.6×10^{16}
p-Al$_{0.15}$Ga$_{0.85}$N/i-Al$_{0.05}$Ga$_{0.95}$N	1.7×10^{16}
p-GaN/p-Al$_{0.15}$Ga$_{0.85}$N	-2.5×10^{16}

3 Simulation results and discussion

The energy band of structure A at forward voltage of 3.4 V is plotted in Fig. 2(a), which uses the interface between the last barrier and EBL as the reference point and so are other figures shown below. It is observed that the quasi-Fermi level of holes around the active region is far away from the valence band edge, indicating that the population of holes injected into the active region is small. This is due to the large effective barrier height for holes injection (~0.423 eV) caused by valence band downward bending which

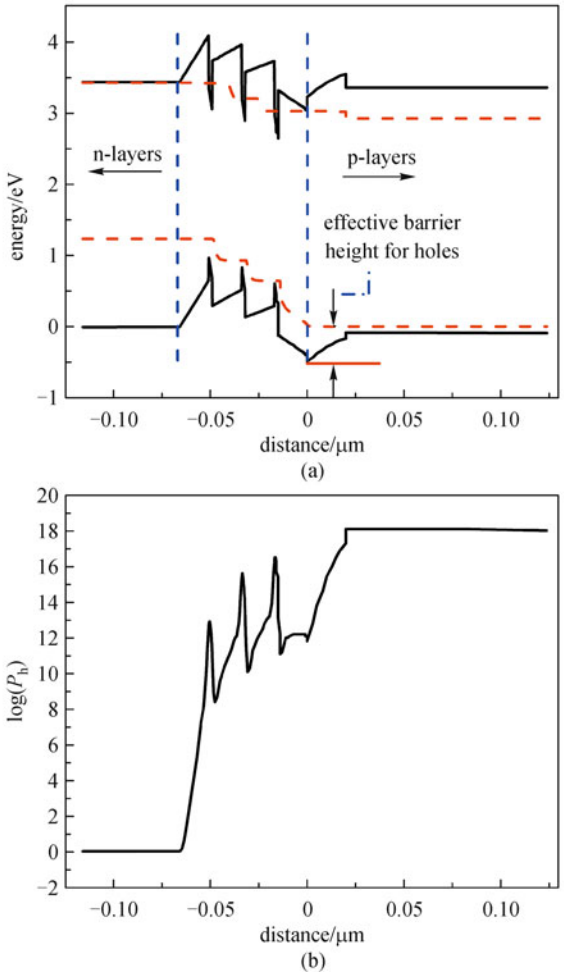

Fig. 2 (a) Energy band diagram of structure A at forward voltage of 3.4 V. The red dash lines indicate the quasi-Fermi levels; (b) distribution of hole concentration P_h in structure A at 3.4 V forward voltage in log scale

results from large polarization field at the interface. Furthermore, because of large effective mass of holes, it is hard for holes to pass through the GaN barriers, resulting in fewer holes in the quantum wells near the n-type layers, which can be seen from Fig. 2(b). As addressed in our approach, the structure with gradually increased barrier heights exhibits better performance in this aspect, which is shown in Fig. 3.

Figure 3(a) shows the energy band diagram of structure B at forward voltage of 3.4 V. Obviously, the polarization at the interface between the last barrier and EBL is decreased, resulting in less downward band bending. As a result, the effective potential height for holes injection is lowered (from 0.423 to 0.312 eV). From this diagram, it is also evident that the hole quasi-Fermi level is nearer to the valence band than that of structure A, resulting in larger hole concentration in QWs. As shown in Fig. 3(b), holes are distributed uniformly in the active region to the concentration of ~10^{19} cm^{-3}, about three orders of magnitude higher than structure A. There are two factors

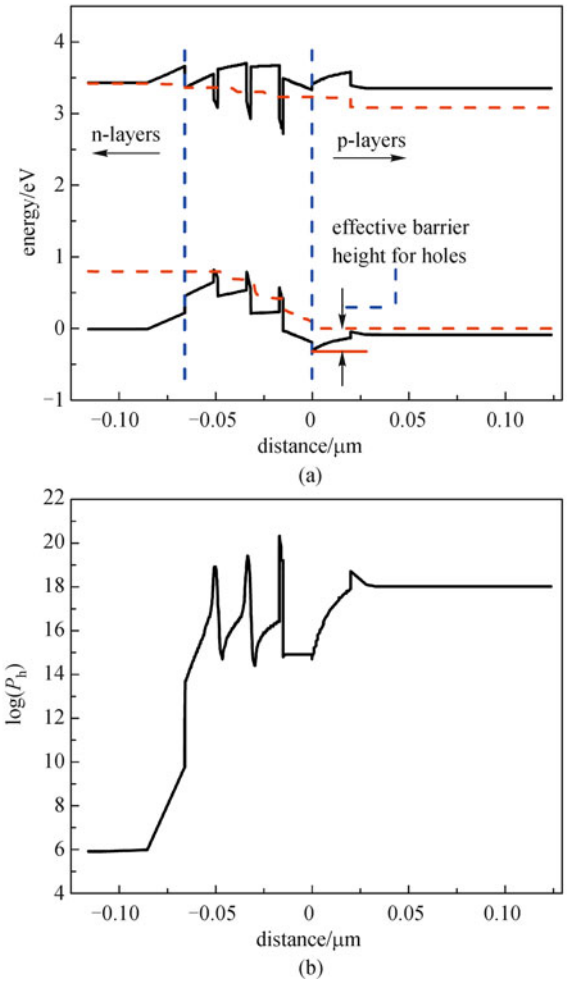

Fig. 3 (a) Energy band diagram of structure B at forward voltage of 3.4 V. The red dash lines indicate the quasi-Fermi levels; (b) distribution of hole concentration P_h in structure B at forward voltage of 3.4 V in log scale

contributing to this improvement. First, due to gradually decreased barrier heights from p-layers to n-layers, holes can be transported from p-type layers to the wells near n-type layers more easily, which contributes to a large number of holes resided in the wells near n-type layers at low voltage. Secondly, because of different composition of In(Al)GaN materials used as barriers, the degree of abrupt change of polarization is lowered, which leads to less fixed charges at the interface between the last barrier and the EBL. It reduces the interface electrostatic field in structure B in comparison with structure A, and so is the field in the last well as dictated by zero-bias boundary condition. As a result, the effective barrier height for hole transport is reduced.

To examine this aspect, we calculate the electrostatic field across the last barrier/EBL interface, and the result is shown in Fig. 4. It can be clearly seen that the electrostatic field at the interface is decreased, and thus the downward band bending is mitigated. Therefore, holes are injected to the active region in structure B with much higher efficiency. The result suggests the importance of minimizing the polarization field in improving the performance of LEDs. It is worth noticing that an effective way of minimizing the electrostatic field in the QW layer is by applying non/semi-polar InGaN QWs [34,35], or polar QWs with large wavefunction overlap design [36,37]. Further investigations will be conducted on the function of gradually increased barrier heights in non-polar InGaN LED devices.

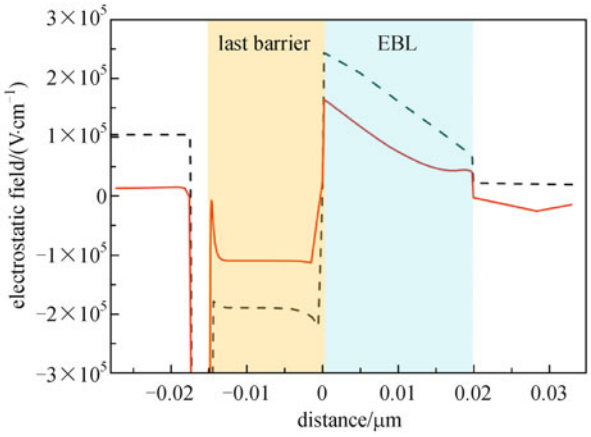

Fig. 4 Electrostatic field in structure A (black dash line) and structure B (red solid line) near the EBL at forward voltage of 3.4 V

Regarding the influence of gradually increased barrier height for MQWs in the active region, we probe into the internal quantum efficiency of both structures. As shown in Fig. 5, the IQE of structure B is also higher than structure A. Since the interface electrostatic field in structure B is smaller than that of structure A, the conduction band bending is mitigated, which means the effective barrier height for electron escape is increased. Because fewer

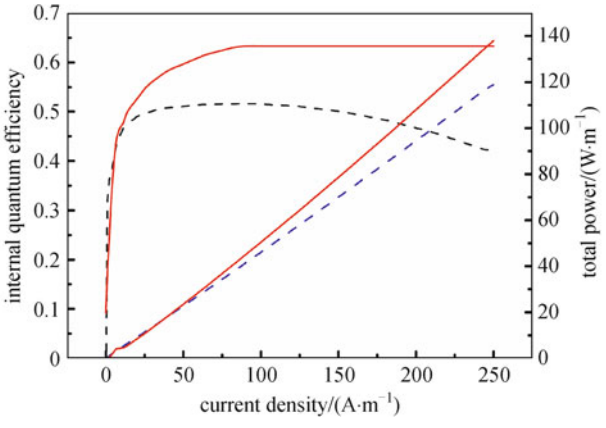

Fig. 5 Total light power and IQE as function of current for structure A (black dash line) and structure B (red solid line)

electrons pass through the EBL, it leads to higher IQE of structure B. As a result, the total output light power of structure B also becomes higher. At the current density of 250 A/m, the total power of structure B is about 27% larger than structure A, which suggests that radiative recombination is more efficient in structure B.

In addition, the total rates of spontaneous emission of these two structures are investigated. As shown in Fig. 6, the spontaneous emission rate of structure B is almost three orders of magnitude higher than structure A, which is resulted from the higher hole concentration in structure B. Furthermore, the full width at half maximum (FHWM) of the emission peak for structure B is 22 nm, slightly larger than that of structure A (18 nm). This can be attributed to the fact that the barrier heights of the QWs in structure B are not uniform, which leads to different transition wavelength in each well. However, the broadening of emission peak is minor such that it does not undermine the application of the proposed structure in blue and white lighting devices.

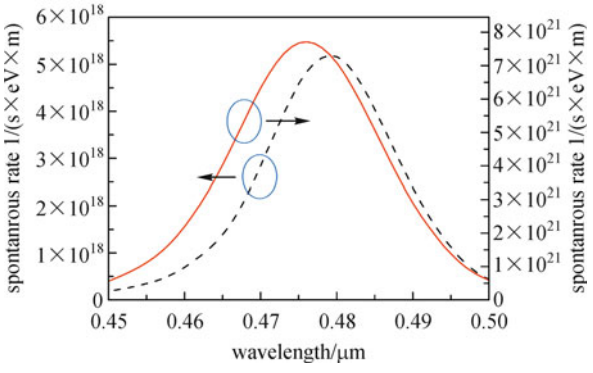

Fig. 6 Total spontaneous emission rate for structure A (black dash line) and structure B (red solid line)

From the above discussion, it is clear that structure B performs better than structure A in both optical and electrical aspects. Compared with the method of Mg doping in the MQWs [23] used for higher hole injection efficiency, the dopant can introduce thread dislocations and stacking dislocations in the active region. In this sense, the approach of gradually-increasing barrier height instead of Mg-doping can not only enhance the hole injection efficiency, but also avoid the problem of poor crystalline quality caused by doping. Therefore, the design of variable barrier height in the active region is preferable for high power and high efficiency light emitting applications. However, this approach requires further growth optimization in realizing the potential advantages.

4 Conclusions

In summary, the effects of barrier height variation on the performance of InGaN LED structure are studied by designing a sample with the active region of gradually increased barrier heights from n- to p-layers. The simulation results show that, when the GaN barriers are replaced by In(Al)GaN materials with increased barrier heights, the degree of abrupt change of polarization at the EBL/last barrier interface is mitigated due to lower lattice mismatch, and holes are injected more efficiently. Furthermore, decreased barrier heights from p-type to n-type layers enhance holes flow in the active region and distribute uniformly. As a result, the designed LED structure shows higher light output power and IQE, which is promising for high efficiency solid-state lighting and other optoelectronic applications.

Acknowledgements This work was supported by the National Natural Science Foundation of China (Grant Nos. 60976042 and 10990103), the National Basic Research Program of China (Nos. 2010CB923204 and 2012CB619302), and the China Postdoctoral Science Foundation (No. 20100480064). The authors are also grateful to Mr. M. Yang from Crosslight Software Inc. for technical assistance.

References

1. Oh J H, Oh J R, Park H K, Sung Y G, Do Y R. New paradigm of multi-chip white LEDs: combination of an InGaN blue LED and full down-converted phosphor-converted LEDs. Optics Express, 2011, 19(Suppl 3): A270–A279
2. Li J, Lin J Y, Jiang H X. Growth of III-nitride photonic structures on large area silicon substrates. Applied Physics Letters, 2006, 88(17): 171909
3. Liao C T, Tsai M C, Liou B T, Yen S H, Kuo Y K. Improvement in output power of a 460 nm InGaN light-emitting diode using staggered quantum well. Journal of Applied Physics, 2010, 108(6): 063107
4. Gao H Y, Yan F W, Zhang Y, Li J M, Zeng Y P, Wang G H. Enhancement of the light output power of InGaN/GaN light-emitting diodes grown on pyramidal patterned sapphire substrates in the micro- and nanoscale. Journal of Applied Physics, 2008, 103(1): 014314
5. Lee J H, Lee D Y, Oh B W, Lee J H. Comparison of InGaN-based LEDs grown on conventional sapphire and cone-shape-patterned sapphire substrate. IEEE Transactions on Electron Devices, 2010, 57(1): 157–163
6. Tansu N, Mawst L J. Current injection efficiency of InGaAsN quantum-well lasers. Journal of Applied Physics, 2005, 97(5): 054502
7. Choi S, Ji M H, Kim J, Kim H J, Satter M M, Yoder P D, Ryou J H, Dupuis R D, Fischer A M, Ponce F A. Efficiency droop due to electron spill-over and limited hole injection in III-nitride visible light-emitting diodes employing lattice-matched InAlN electron blocking layers. Applied Physics Letters, 2012, 101(16): 161110
8. Hori A, Yasunaga D, Satake A, Fujiwara K. Temperature and injection current dependence of electroluminescence intensity in green and blue InGaN single-quantum-well light-emitting diodes.

Journal of Applied Physics, 2003, 93(6): 3152–3157
9. Wang C H, Chang S P, Ku P H, Li J C, Lan Y P, Lin C C, Yang H C, Kuo H C, Lu T C, Wang S C, Chang C Y. Hole transport improvement in InGaN/GaN light-emitting diodes by graded-composition multiple quantum barriers. Applied Physics Letters, 2011, 99(17): 171106
10. Otsuji N, Fujiwara K, Sheu J K. Electroluminescence efficiency of blue InGaN/GaN quantum-well diodes with and without an n-InGaN electron reservoir layer. Journal of Applied Physics, 2006, 100(11): 113105
11. Zhao H P, Liu G Y, Arif R A, Tansu N. Current injection efficiency induced efficiency-droop in InGaN quantum well light-emitting diodes. Solid-State Electronics, 2010, 54(10): 1119–1124
12. Zhao H P, Liu G Y, Zhang J, Arif R A, Tansu R. Analysis of internal quantum efficiency and current injection efficiency in III-nitride light-emitting diodes. Journal of Display Technology, 2013, 9(4): 212–225
13. Titkov I E, Sannikov D A, Park Y M, Son J K. Blue light emitting diode internal and injection efficiency. AIP Advances, 2012, 2(3): 032117
14. Xu L F, Patel D, Menoni C S, Yeh J Y, Mawst L J, Tansu N. Experimental evidence of the impact of nitrogen on carrier capture and escape times in InGaAsN/GaAs single quantum well. IEEE Photonics Journal, 2012, 4(6): 2262–2271
15. Tansu N, Mawst L J. The role of hole leakage in 1300-nm InGaAsN quantum-well lasers. Applied Physics Letters, 2003, 82(10): 1500–1502
16. Chang J Y, Tsai M C, Kuo Y K. Advantages of blue InGaN light-emitting diodes with AlGaN barriers. Optics Letters, 2010, 35(9): 1368–1370
17. Liu G Y, Zhang J, Tan C K, Tansu N. Efficiency-droop suppression by using large-bandgap AlGaInN thin barrier layers in InGaN quantum-well light-emitting diodes. IEEE Photonics Journal, 2013, 5(2): 2201011
18. Delaney K T, Rinke P, Van de Walle C G. Auger recombination rates in nitrides from first principles. Applied Physics Letters, 2009, 94(19): 191109
19. Tan C K, Zhang J, Li X H, Liu G Y, Tayo B O, Tansu N. First-principle electronic properties of dilute-As GaNAs alloy for visible light emitters. Journal of Display Technology, 2013, 9(4): 272–279
20. Kuo Y K, Chang J Y, Tsai M C. Enhancement in hole-injection efficiency of blue InGaN light-emitting diodes from reduced polarization by some specific designs for the electron blocking layer. Optics Letters, 2010, 35(19): 3285–3287
21. Kuo Y K, Tsai M C, Yen S H. Numerical simulation of blue InGaN light-emitting diodes with polarization-matched AlGaInN electron-blocking layer and barrier layer. Optics Communications, 2009, 282 (21): 4252–4255
22. Zhang Y Y, Yin Y A. Performance enhancement of blue light-emitting diodes with a special designed AlGaN/GaN superlattice electron-blocking layer. Applied Physics Letters, 2011, 99(22): 221103
23. Vampola K J, Iza M, Keller S, DenBaars S P, Nakamura S. Measurement of electron overflow in 450 nm InGaN light-emitting diode structures. Applied Physics Letters, 2009, 94(6): 061116-1–061116–3
24. Liou B T, Tsai M C, Liao C T, Yen S H, Kuo Y K. Numerical investigation of blue InGaN light-emitting diodes with staggered quantum wells. Proceedings of the Society for Photo-Instrumentation Engineers, 2009, 7211: 72111D-1–72111D-8
25. Jain S C, Willander M, Narayan J, Overstraeten R V. III–nitrides: growth, characterization, and properties. Journal of Applied Physics, 2000, 87(3): 965–1006
26. Yen S H, Kuo Y K. Polarization-dependent optical characteristics of violet InGaN laser diodes. Journal of Applied Physics, 2008, 103 (10): 103115-1–103115-6
27. Kuo Y K, Yen S H, Wang Y W. Simulation of deep ultraviolet light-emitting diodes. Proceedings of the Society for Photo-Instrumentation Engineers, 2007, 6669: 66691J
28. Ambacher O, Foutz B, Smart J, Shealy J R, Weimann N G, Chu K, Murphy M, Sierakowski A J, Schaff W J, Eastman L F, Dimitrov R, Mitchell A, Stutzmann M. Two dimensional electron gases induced by spontaneous and piezoelectric polarization in undoped and doped AlGaN/GaN hetero-structures. Journal of Applied Physics, 2000, 87 (1): 334–344
29. Fiorentini V, Bernardini F, Ambacher O. Evidence for nonlinear macroscopic polarization in III–V nitride alloy heterostructures. Applied Physics Letters, 2002, 80(7): 1204–1206
30. Ridley B K, Schaff W J, Eastman L F. Theoretical model for polarization superlattices: Energy levels and intersubband transitions. Journal of Applied Physics, 2003, 94(6): 3972–3978
31. Vurgaftman I, Meyer J R. Band parameters for nitrogen-containing semiconductors. Journal of Applied Physics, 2003, 94(6): 3675–3696
32. Vurgaftman I, Meyer J R, Ram-Mohan L R. Band parameters for III–V compound semiconductors and their alloys. Journal of Applied Physics, 2001, 89(11): 5815–5875
33. Chichibu S F, Abare A C, Minsky M S, Keller S, Fleischer S B, Bowers J E, Hu E, Mishra U K, Coldren L A, DenBaars S P, Sota T. Effective band gap inhomogeneity and piezoelectric field in InGaN/GaN multiquantum well structures. Applied Physics Letters, 1998, 73(14): 2006–2008
34. Feezell D F, Speck J S, DenBaars S P, Nakamura S. Semipolar (20-2-1) InGaN/GaN light-emitting diodes for high-efficiency solid-state lighting. Journal of Display Technology, 2013, 9(4): 190–198
35. Farrell R M, Haeger D A, Fujito K, DenBaars S P, Nakamura S, Speck J S. Morphological evolution of InGaN/GaN light-emitting diodes grown on free-standing *m*-plane GaN substrates. Journal of Applied Physics, 2013, 113(6): 063504
36. Zhang J, Tansu N. Optical gain and laser characteristics of InGaN quantum wells on ternary InGaN substrates. IEEE Photonics Journal, 2013, 5(2): 2600111
37. Zhao H P, Liu G Y, Zhang J, Poplawsky J D, Dierolf V, Tansu N. Approaches for high internal quantum efficiency green InGaN light-emitting diodes with large overlap quantum wells. Optics Express, 2011, 19(Suppl 4): A991–A1007